ARTICLE     OPEN

# Nrf2 signaling activation by a small molecule activator compound 16 inhibits hydrogen peroxide-induced oxidative injury and death in osteoblasts

Jing-wei Zhao[1,7], Pei-jun Tang[2,7], Zhen-tao Zhou[3,7], Gang Xu[3], Quan Li [ID][4✉], Ke-ran Li [ID][5✉] and Yue-huan Zheng [ID][6✉]

We explored the potential activity of compound 16 (Cpd16), a novel small molecule Nrf2 activator, in hydrogen peroxide ($H_2O_2$)-stimulated osteoblasts. In the primary murine/human osteoblasts and MC3T3-E1 murine osteoblastic cells, Cpd16 treatment at micro-molar concentrations caused disassociation of Keap1-Nrf2 and Nrf2 cascade activation. Cpd16 induced stabilization of Nrf2 protein and its nuclear translocation, thereby increasing the antioxidant response elements (ARE) reporter activity and Nrf2 response genes transcription in murine and human osteoblasts. Significantly, Cpd16 mitigated oxidative injury in $H_2O_2$-stimulited osteoblasts. $H_2O_2$-provoked apoptosis as well as programmed necrosis in osteoblasts were significantly alleviated by the novel Nrf2 activator. Cpd16-induced Nrf2 activation and osteoblasts protection were stronger than other known Nrf2 activators. Dexamethasone- and nicotine-caused oxidative stress and death in osteoblasts were attenuated by Cpd16 as well. Cpd16-induced osteoblast cytoprotection was abolished by Nrf2 short hairpin RNA or knockout, but was mimicked by Keap1 knockout. Keap1 Cys151S mutation abolished Cpd16-induced Nrf2 cascade activation and osteoblasts protection against $H_2O_2$. Importantly, weekly Cpd16 administration largely ameliorated trabecular bone loss in ovariectomy mice. Together, Cpd16 alleviates $H_2O_2$-induced oxidative stress and death in osteoblasts by activating Nrf2 cascade.

## INTRODUCTION

Osteoporosis and osteonecrosis are extremely common systemic bone diseases that are characterized by significantly decreased bone mass as well as progressive architectural deterioration in the bone [1–3]. Studies have implied that excessive reactive oxygen species (ROS) and oxidative cell injury are the major contributors for the development and progression of osteoporosis and osteonecrosis [4–6]. Specifically, ROS can lead to profound oxidative injury to osteoblasts [7–9]. Hydrogen peroxide ($H_2O_2$) and other oxidative stimuli (dexamethasone, nicotine and etc.) are added to osteoblasts/osteoblastic cells [10–16]. These stimuli can led to significant oxidative injury and robust death of osteoblasts [11–14, 16].

Nrf2 drives the transcription of a significant number of antioxidant and cytoprotective genes, through association with a *cis*-acting element (ARE/EpRE) in the promoter region in the nuclei [17–21]. In the resting condition, however, Nrf2 is negatively regulated by Keap1, the latter initiates poly-ubiquitination and degradation machinery to promote Nrf2 protein degradation and stops Nrf2 translocation into cell nuclei [18, 19]. Therefore small molecules that block the Keap1-Nrf2 binding should extent the Nrf2's half-life, stabilizing Nrf2 protein, causing its accumulation in cytosol and subsequent translocation to nuclei, thereby activating Nrf2 signaling cascade [17–21].

Pharmacological or genetic activation of Nrf2 cascade can efficiently protect osteoblasts/osteoblastic cells against oxidative injury by $H_2O_2$ [10, 13, 15, 16, 22–24] and other oxidative stimuli [25–29]. We have previously shown that four-octyl itaconate (4-OI) activated Nrf2 cascade through alkylating Keap1's cysteine residues and potently inhibited $H_2O_2$-induced osteoblast death [10]. Moreover, iKeap1, a direct and novel Keap1 inhibitor that was discovered by the structure-based virtual screening, inhibited $H_2O_2$-induced osteoblast death by activating Nrf2 signaling cascade [30]. In addition, MIND4-17, the novel activator that uniquely activated Nrf2 signaling cascade by separating Nrf2-Keap1 complex, protected osteoblasts from $H_2O_2$-induced oxidative injury and death [16]. Chlorogenic acid significantly attenuated $H_2O_2$-caused oxidative stress and death in MC3T3-E1 osteoblastic cells by activating Nrf2 signaling cascade [15].

Genetic strategies were also utilized to activate Nrf2 signaling cascade. microRNA-455 (miR-455) silenced Cullin 3, thereby activating Nrf2 signaling and protecting osteoblasts against oxidative stress [13]. Liang et al. have recently shown that a novel microRNA, microRNA-4523, silenced phosphoglycerate kinase 1

[1]Division of Spine Surgery, Department of Orthopedics, Tongji Hospital, Tongji University School of Medicine, Shanghai, China. [2]Department of Pulmonary, The Affiliated Infectious Hospital of Soochow University, Suzhou, China. [3]Department of Orthopedics, The Second Affiliated Hospital of Soochow University, Suzhou, China. [4]Center of Stomatology, The Second Affiliated Hospital of Soochow University, Suzhou, China. [5]The Fourth School of Clinical Medicine, The Affiliated Eye Hospital, Nanjing Medical University, Nanjing, China. [6]Department of Orthopedics, Ruijin Hospital, Shanghai Jiao Tong University School of Medicine, Shanghai, China. [7]These authors contributed equally: Jing-wei Zhao, Pei-jun Tang, Zhen-tao Zhou. ✉email: liquan84@163.com; likeran@njmu.edu.cn; zyh12693@rjh.com.cn

(PGK1) to stimulate Nrf2 signaling, protecting human osteoblasts from dexamethasone-caused oxidative injury [31]. Other Nrf2-activating miRNAs, including miR-200a [28], miR-107 [32], and miR-19a [26], also offered significant osteoblast cytoprotection by suppressing oxidative injury.

Marcotte et al. have recently developed a small molecule inhibitor of Nrf2-Keap1 interaction named compound 16 (Cpd16, PubChem CID 1073725) [33]. Cpd16 binds directly to the Keap1's Kelch-DC domain at the C-terminus of Keap1 with the $IC_{50}$ of 2.7 μM [33]. It was able to increase Nrf2 response genes in cultured cells and acted as a novel Nrf2 activator [33]. Here our study reported that Cpd16 activated Nrf2 cascade and protected osteoblasts from $H_2O_2$.

## RESULTS

### Cpd16 activates Nrf2 signaling cascade in osteoblasts

As shown, Cpd16 dose-dependently enhanced ARE luciferase reporter activity in murine osteoblasts (Fig. 1A). Further indicating Nrf2 cascade activation, NQO1 enzyme activity was remarkably increased after 1–25 μM of Cpd16 treatment (Fig. 1A). Cpd16 at 0.2 μM failed to significantly increase the NQO1 enzyme activity, showing the dose-dependent response (Fig. 1A). CCK-8 assay results found that Cpd16 (0.2–25 μM, for 24 h) failed to significantly decrease the viability in murine osteoblasts (Fig. 1A), suggesting that the compound is relatively safe to murine osteoblasts. At the two concentrations, 5 μM and 25 μM, Cpd16 robustly increased ARE reporter activity and the NQO1 enzyme activity in murine osteoblasts (Fig. 1A), they were selected for the following experiments.

Treatment with Cpd16 (5 μM and 25 μM for 2 h) disrupted association of Keap1-Nrf2 in primary murine osteoblasts (Fig. 1B). As a result, the cytosol Nrf2 protein levels were significantly increased (Fig. 1C). On the contrary, Cpd16 failed to significantly alter Keap1 protein (Fig. 1C) and *Nrf2* mRNA expression (Fig. 1D) in murine osteoblasts. These results implied that Cpd16 induced Keap1-Nrf2 departure and stabilization of Nrf2 protein in murine osteoblasts. Notably, Cpd16 (25 μM) was unable to further increase Nrf2 protein levels in murine osteoblasts with MG-132 co-treatment (Fig. 1E). Moreover, cycloheximide (CHX), the known protein synthesis inhibitor [34], did not alter Nrf2 protein expression in Cpd16 (25 μM)-treated primary murine osteoblasts (Fig. 1F). These results further supported Nrf2 protein stabilization following Cpd16 treatment in cultured osteoblasts.

Stabilized Nrf2 protein translocated from cytosol to nuclei of the murine osteoblasts (Fig. 1G), which is an initial and key step for activation of the Nrf2 cascade [18, 19, 35]. Indeed, Nrf2-transcripted genes, including *HO1*, *GCLC,* and *NQO1* [10, 16, 28, 30, 36], were remarkably elevated following Cpd16 (5/25 μM) treatment (Fig. 1H). Their protein levels, tested by Western blotting assays, were increased as well (Fig. 1I).

In human osteoblasts [10, 30], 25 μM of Cpd16 treatment disrupted Keap1 immunoprecipitation with Nrf2 (Fig. 1J) as well, leading to stabilization of Nrf2 protein in cytosol (Fig. 1K). Keap1 protein (Fig. 1K) and *Nrf2* mRNA (Fig. 1L) were not significantly changed. After testing the nuclear fraction lysates, we showed that the accumulated Nrf2 protein translocated to the nuclei (Fig. 1M). Consequently, expression of Nrf2 response genes were significantly increased (Fig. 1N, O). Similarly in MC3T3-E1 murine osteoblastic cells, Cpd16 treatment stabilization Nrf2 protein (Fig. 1P) and increased mRNA expression of Nrf2 response genes (Fig. 1Q). Together, Cpd16 activated Nrf2 signaling in osteoblasts.

### Cpd16 ameliorates $H_2O_2$-provoked oxidative injury in osteoblasts

By measuring the CellROX fluorescence intensity, we demonstrated that $H_2O_2$ induced robust ROS production (CellROX intensity increase) in the primary murine osteoblasts (Fig. 2A, B).

Significantly, pretreatment with Cpd16 (5/25 μM) potently inhibited $H_2O_2$-induced ROS production (Fig. 2A, B). Moreover, $H_2O_2$-induced lipid peroxidation, or TBAR activity increase, was largely inhibited by Cpd16 pretreatment as well (Fig. 2C). In addition, in murine osteoblasts the novel Nrf2 activator largely attenuated $H_2O_2$-induced mitochondrial depolarization (tested by the formation of JC-1 monomers, Fig. 2D, E). ssDNA accumulation indicated enhanced DNA breaks in $H_2O_2$-treated murine osteoblasts (Fig. 2F), which was suppressed by Cpd16 pretreatment (Fig. 2F).

Pretreatment with Cpd16 (25 μM) in the primary human osteoblasts significantly ameliorated $H_2O_2$-stimulated ROS production (Fig. 2G, H) and mitochondrial depolarization (formation of JC-1 monomer, Fig. 2I, J). In MC3T3-E1 murine osteoblastic cells, pretreatment with Cpd16 also potently inhibited $H_2O_2$-stimulated ROS production (Fig. 2K, L). Thus, Cpd16 ameliorated $H_2O_2$-induced oxidative injury in osteoblasts.

### Cpd16 ameliorates $H_2O_2$-induced apoptosis and programmed necrosis in osteoblasts

$H_2O_2$ will cause death of cultured osteoblasts [10, 13, 16, 22, 30, 37, 38]. In line with our previous findings [10, 30], $H_2O_2$ exerted pro-apoptotic activity in cultured murine osteoblasts, as it increased the caspase-3/-9 activities (Fig. 3A, B) and caused caspase-3 and PARP cleavages (Fig. 3C), which were ameliorated by pretreatment of Cpd16 (5/25 μM). $H_2O_2$ provoked apoptosis in murine osteoblasts, increasing Annexin-positive staining cells (Fig. 3D) and TUNEL-nuclei staining (Fig. 3E). Cpd16 potently reduced $H_2O_2$-induced apoptosis activation in murine osteoblasts (Fig. 3D, E). Moreover, $H_2O_2$-induced cytotoxicity or CCK-8 viability reduction (Fig. 3F), was alleviated by Cpd16 as well.

Besides apoptosis, studies have shown that $H_2O_2$ together other oxidative stimuli could simultaneously provoke programmed necrosis cascade [10, 13, 30, 39, 40]. It is a mitochondria-dependent active cell necrosis cascade that can be initiated by mitochondrial CyPD (cyclophilin D)-ANT1 (ADP/ATP translocase 1)-p53 association [41–43]. $H_2O_2$ (400 μM, 4 h) stimulation in murine osteoblasts indeed induced CyPD-ANT1-p53 association in the mitochondria [10, 30], and pretreatment with Cpd16 (5/25 μM) significantly inhibited the complex formation (Fig. 3G). To supporting necrosis induction, medium LDH levels were increased following $H_2O_2$ treatment in murine osteoblasts (Fig. 3H), which was again inhibited by Cpd16 (Fig. 3H). These results supported that the novel Nrf2 activator also inhibited programmed necrosis cascade activation in murine osteoblasts.

In the primary human osteoblasts pretreatment with Cpd16 dramatically inhibited $H_2O_2$-induced caspase-3-apoptosis activation (Fig. 3I–K). Apoptosis induction was evidenced by the quantified results from Annexin-V flow cytometry (Fig. 3J) and TUNEL nuclei staining (Fig. 3K) assays. In addition, pretreatment with Cpd16 (25 μM) inhibited $H_2O_2$-induced viability reduction (Fig. 3L). Furthermore, $H_2O_2$-induced mitochondrial association of CyPD-ANT1-p53 (Fig. 3M) and LDH releasing (Fig. 3N) were significantly inhibited by the novel Nrf2 activator in human osteoblasts. In MC3T3-E1 osteoblastic cells, $H_2O_2$-induced apoptosis (TUNEL assays, Fig. 3O) and necrosis (Fig. 3P) were inhibited by Cpd16 pretreatment as well.

### Cpd16-induced Nrf2 activation and osteoblasts protection against $H_2O_2$ were stronger than other known Nrf2 activators

The activity of Cpd16 was compared to other known Nrf2 activators, including 4-OI [10, 44, 45], SFH [46, 47], and TBHQ [48, 49]. At shown in the primary murine osteoblasts, at the same concentration (25 μM), Cpd16-induced increases in ARE activity (Fig. 4A) and *HO1* expression (Fig. 4B) were significantly more potent than these other Nrf2 activators (4-OI, SFH, and TBHQ). Importantly, although each of the applied Nrf2 activators ameliorated $H_2O_2$-caused viability decreasing (Fig. 4C), apoptosis
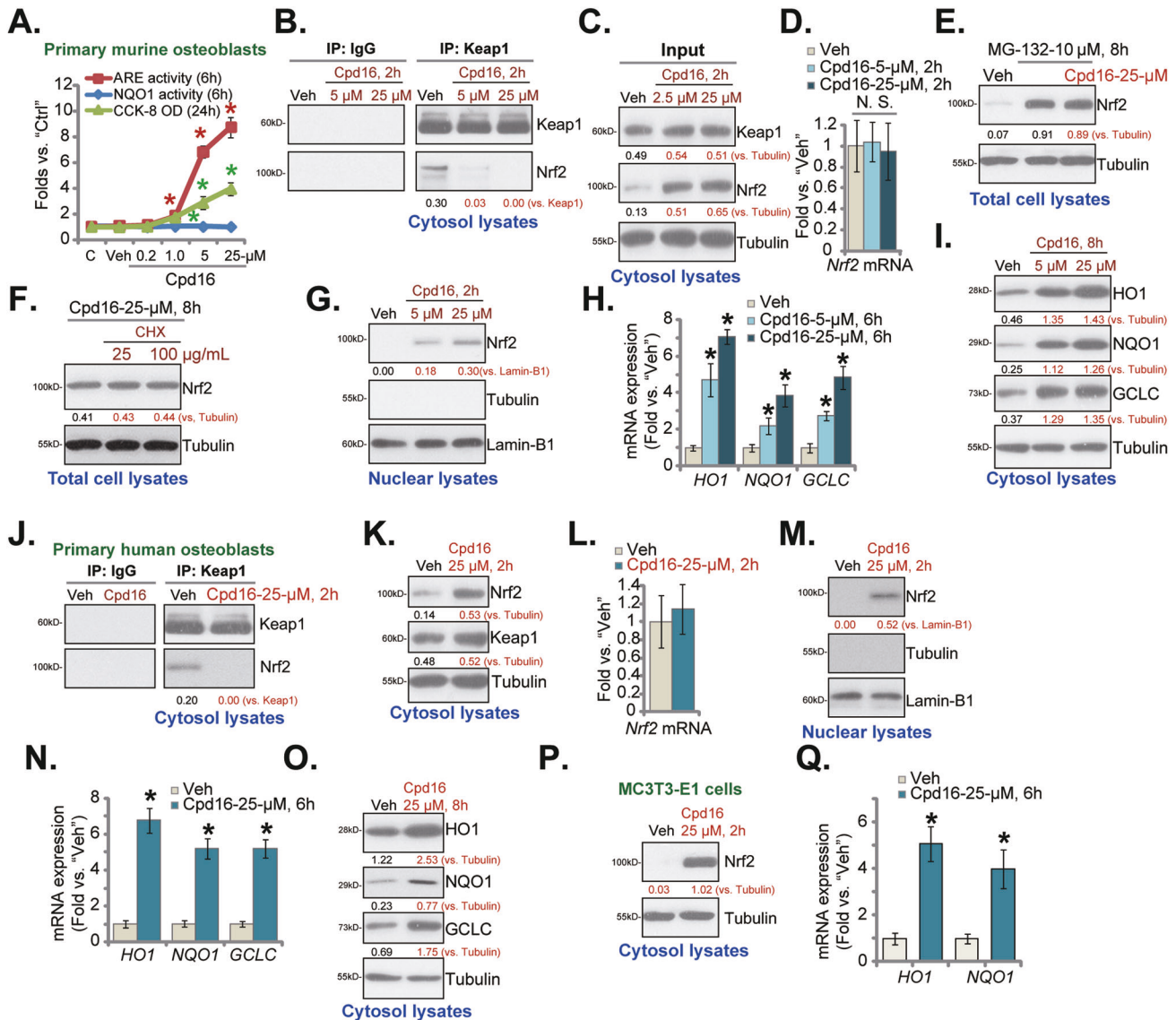
**Fig. 1 Cpd16 activates Nrf2 signaling cascade in osteoblasts.** Primary murine osteoblasts (**A–D, G–I**), human osteoblasts (**J–O**), or the MC3T3-E1 murine osteoblastic cells (**P, Q**) were stimulated with Cpd16, ARE activity and NQO1 activity as well as cell viability were measured (**A**); Keap1-Nrf2 association was measured through co-immunoprecipitation (Co-IP) (**B, J**); Proteins in cytosol/nuclear fraction lysates were examined (**C, G, I, K, M, O, P**), with mRNAs measured by qRT-PCR (**D, H, L, N, Q**). The primary murine osteoblasts were treated with MG-132 (10 μM) or plus Cpd16 (25 μM) for 8 h, total protein lysates were tested (**E**). The murine osteoblasts were pretreated for 1 h with cycloheximide (CHX, 25/100 μg/mL), following by Cpd16 (25 μM) stimulation for another 8 h, listed proteins were shown (**F**). "C" is untreated control (same for all Figures). "Veh" is vehicle control (0.1% DMSO) (same for all Figures). *$P < 0.05$ versus "Veh" cells.

(Fig. 4D), and necrosis (LDH releasing, Fig. 4E) in primary murine osteoblasts. Cpd16-mediated osteoblast protection was more significant than these other activators (4-OI, SFH, and TBHQ) (Fig. 4C–E). In human osteoblasts and MC3T3-E1 murine osteoblastic cells, Cpd16-induced *HO1* mRNA expression was again more significant than the same concentration of 4-OI, SFH, or TBHQ (Fig. 4F, G). Therefore, Cpd16-induced Nrf2 activation and osteoblasts protection against $H_2O_2$ were stronger than other known Nrf2 activators.

### Cpd16 inhibits dexamethasone- and nicotine-induced oxidative injury in osteoblasts

Besides $H_2O_2$, other stimuli, including dexamethasone (DEX) [28, 29, 36, 50] and nicotine [30, 51–53], can also provoke oxidative injury in osteoblasts, which could be alleviated by Nrf2. As shown, DEX and nicotine both induced profound oxidative injury, increasing CellROX intensity (Fig. 5A) and JC-1 monomers (Fig. 5B) in murine osteoblasts. Importantly, Cpd16 largely inhibited DEX- and nicotine-induced oxidative stress in murine osteoblasts (Fig. 5A, B). Functional studies demonstrated that the novel Nrf2 activator significantly attenuated cytotoxicity by DEX and nicotine in murine osteoblasts. DEX- and nicotine-induced apoptosis (Fig. 5C), viability decreasing (Fig. 5D), and necrosis (LDH releasing, Fig. 5E) were largely inhibited by Cpd16. In human osteoblasts, DEX-/nicotine-induced oxidative stress (CellROX intensity assays, Fig. 5F), apoptosis (Fig. 5G), viability decreasing (Fig. 5H), and necrosis (Fig. 5I) were ameliorated by Cpd16. In MC3T3-E1 murine osteoblastic cells, Cpd16 treatment potently inhibited DEX- and nicotine-induced viability decreasing (Fig. 5J) and necrosis (Fig. 5K) as well. Thus, Cpd16 inhibited dexamethasone-/nicotine-induced oxidative injury in osteoblasts.
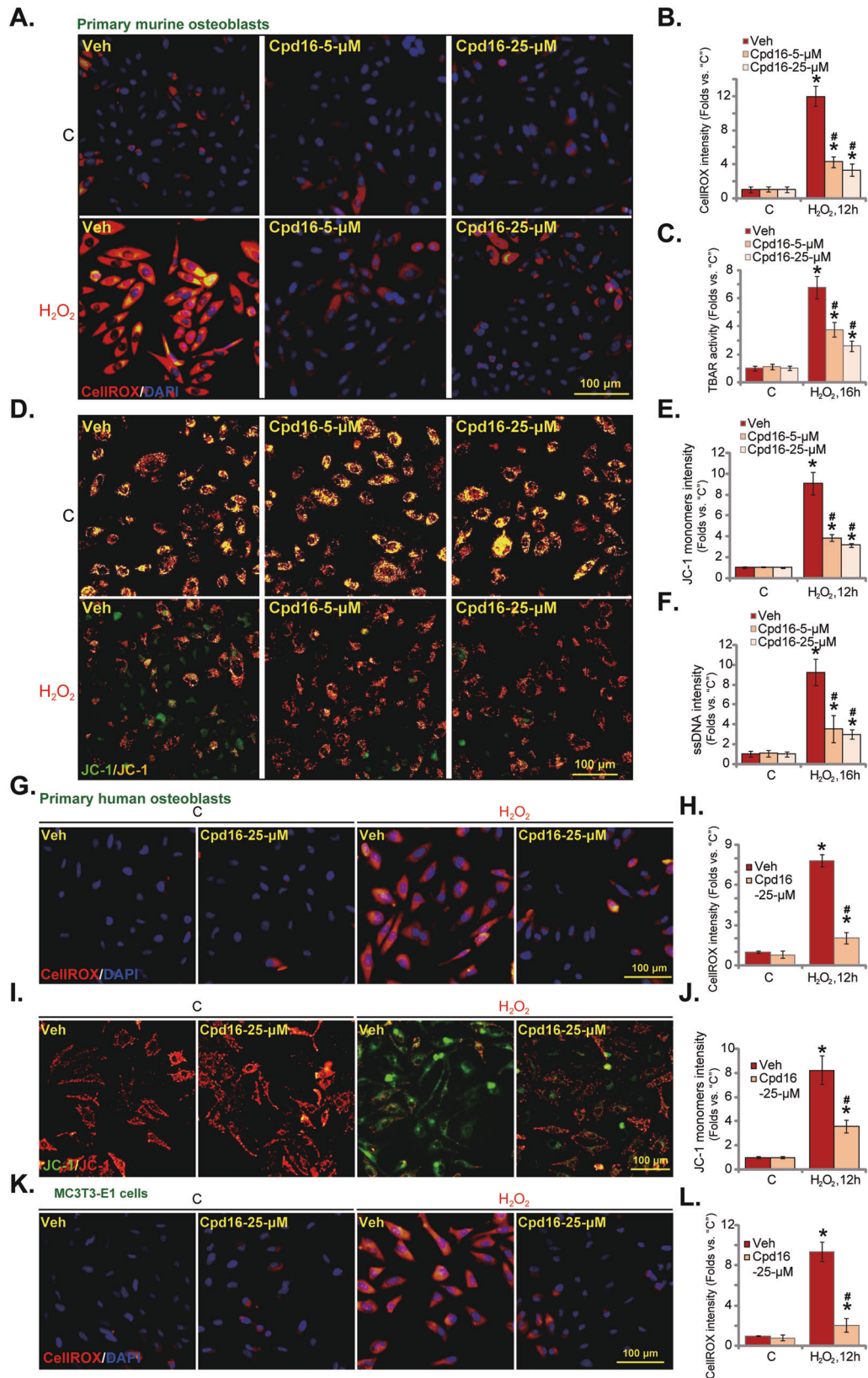
**Fig. 2  Cpd16 ameliorates H$_2$O$_2$-provoked oxidative injury in osteoblasts.** Primary murine osteoblasts (**A–F**), human osteoblasts (**G–J**), or the MC3T3-E1 murine osteoblastic cells (**K** and **L**) were pretreated (for 2 h) with Cpd16 (5/25 μM), or plus H$_2$O$_2$ (400 μM) stimulation; ROS contents (the CellROX intensity assay, **A**, **B**, **G**, **H**, **K**, **L**), TBAR activity (**C**), JC-1 dye staining (**D**, **E**, **I**, **J**), and ssDNA contents (**F**) were measured. *$P < 0.05$ versus "C" cells. #$P < 0.05$ versus cells with H$_2$O$_2$ stimulation but "Veh" pretreatment. Scale bar = 100 μm.
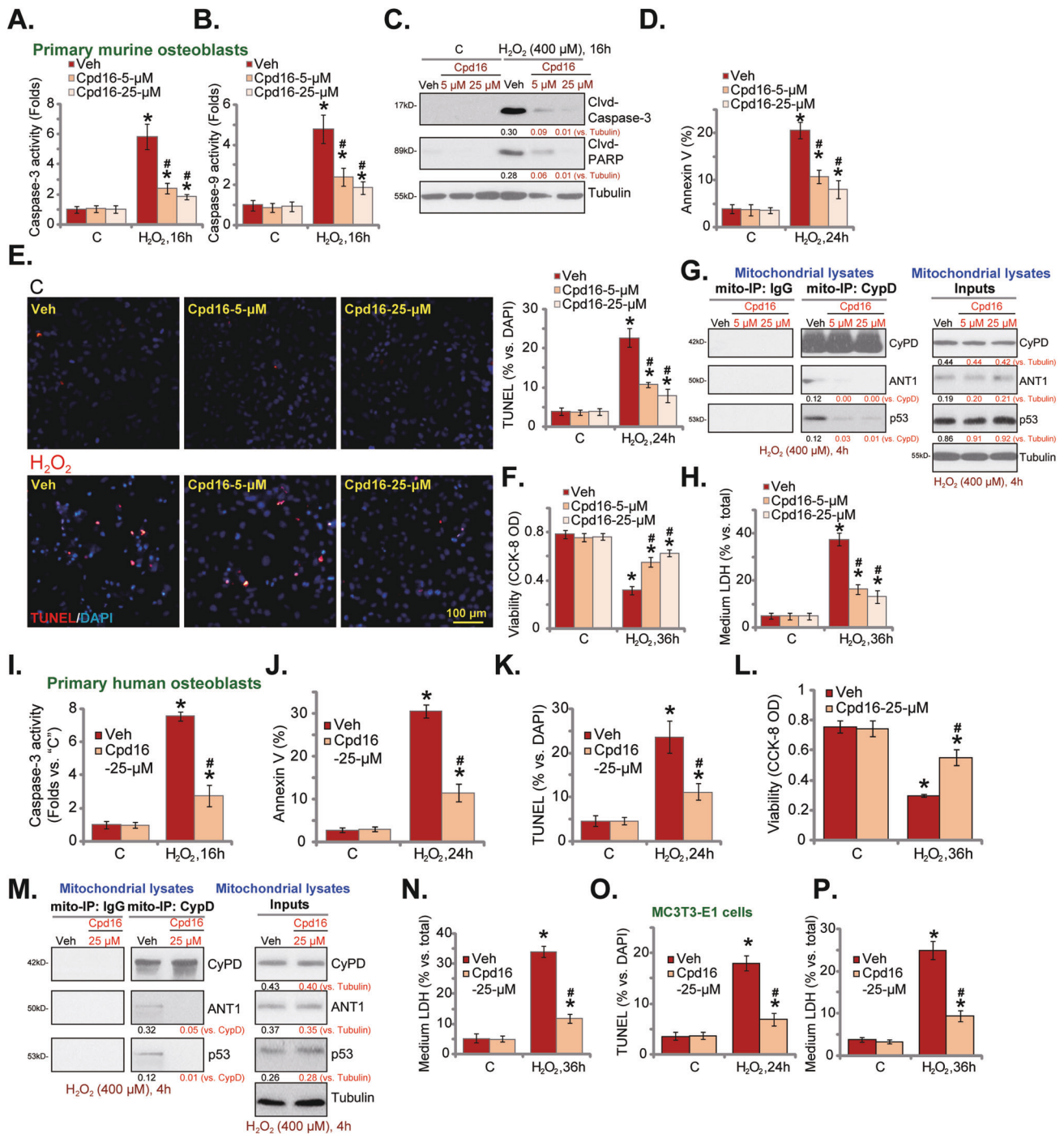
**Fig. 3 Cpd16 ameliorates H₂O₂-induced apoptosis and programmed necrosis in osteoblasts.** Primary murine osteoblasts (**A–H**), human osteoblasts (**I–N**) or the MC3T3-E1 murine osteoblastic cells (**O, P**) were pretreated (for 2 h) with Cpd16 (5/25 μM), or plus H₂O₂ (400 μM) stimulation; the caspase-3/-9 activities (**A, B, I**) were measured; apoptosis-associated proteins were measured (**C**); cell apoptosis was examined by Annexin V flow cytometry (**D, J**, results were quantified) and the nuclear TUNEL staining (**E, K**, and **O**, results were quantified) assays, with cell viability measured through CCK-8 assays (**F, L**); CyPD-ANT1-p53 mitochondrial complexation and the expression were shown (**G, M**), and cell necrosis measured through measuring LDH releasing (**H, N, P**). *$P < 0.05$ versus "C" cells. #$P < 0.05$ versus cells with H₂O₂ stimulation but "Veh" pretreatment. Scale bar = 100 μm.

## Nrf2 activation is indispensable for Cpd16-mediated osteoblast cytoprotection

Genetic strategies were employed to silence Nrf2. Nrf2 shRNA-expressing lentivirus [10, 30] was added to cultured primary murine osteoblasts, and stable osteoblasts were formed after puromycin selection: namely "sh-Nrf2" osteoblasts. Moreover, Nrf2 knockout (KO) osteoblasts were established by transducing the CRISPR/Cas9-Nrf2-KO construct to the Cas9-expressing murine osteoblasts. After selection (through puromycin) and KO screening the single stable Nrf2 KO murine osteoblasts, namely "ko-Nrf2" osteoblasts, were formed. Control cells were with the scramble control shRNA ("shC") plus the CRISPR/Cas9 empty vector ("Cas9-C"). As shown, *Nrf2* mRNA expression (Fig. 6A) and Cpd16 (25 μM, 8 h)-induced Nrf2 protein stabilization (Fig. 6B) were nullified by
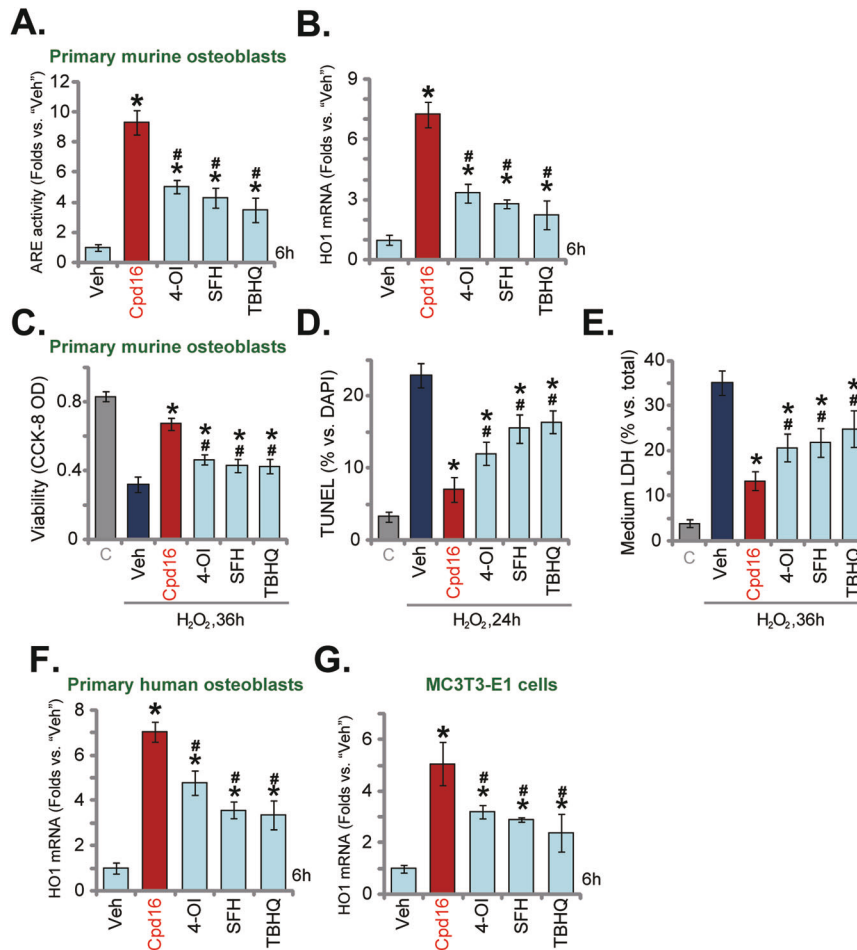
**Fig. 4  Cpd16-induced Nrf2 activation and osteoblasts protection against H₂O₂ were stronger than other known Nrf2 activators.** The primary murine osteoblasts (**A**, **B**), human osteoblasts (**F**), and MC3T3-E1 murine osteoblastic cells (**G**) were treated with 25 μM of Cpd16, Sulforaphane (SFH), 4-octyl itaconate (4-OI), tert-butylhydroquinone (TBHQ), and cultured for 6 h, the relative ARE activity (**A**) and *HO1* mRNA (**B**, **F**, **G**) expression were tested. The primary murine osteoblasts were pretreated with 25 μM of Cpd16, SFH, 4-OI, or TBHQ for 2 h, followed by H₂O₂ (400 μM) stimulation, and viability, apoptosis, and necrosis were measured through CCK-8 (**C**), TUNEL-nuclei staining (**D**), and LDH releasing (**E**) assays, respectively. *$P < 0.05$ *versus* "Veh". #$P < 0.05$. *versus* "Cpd16".

Nrf2 shRNA/KO in murine osteoblasts. Moreover, Cpd16 (25 μM, 8 h)-provoked ARE luciferase reporter activity increase (Fig. 6C), mRNA (Fig. 6D), and protein (Fig. 6B) expression of Nrf2-ARE response genes were almost completely reversed following Nrf2 silencing or KO.

In Nrf2-depleted osteoblasts H₂O₂-caused viability reduction (Fig. 6E), apoptosis (Fig. 6F), and necrosis (LDH releasing, Fig. 6G) were exacerbated, suggesting that the basal Nrf2 activation can attenuate H₂O₂-induced cytotoxicity. More importantly, Cpd16 was completely ineffective against H₂O₂ in Nrf2-depleted murine osteoblasts (Fig. 6E–G). Thus, Nrf2 depletion abolished Cpd16-induced cytoprotective activity in osteoblasts.

We further hypothesized that Cpd16 should be invalid in Nrf2 over-activated osteoblasts. Thus, a described CRISPR/Cas9-Keap1-KO construct [10, 30] was stably transduced to the Cas9-expressing osteoblasts to establish "ko-Keap1" osteoblasts, showing depleted *Keap1* (Fig. 6H, I). Keap1 KO did not affect *Nrf2* mRNA expression in murine osteoblasts (Fig. 6H), but induced robust Nrf2 protein stabilization (Fig. 6I). It also robustly increased expression of Nrf2 response genes (Fig. 6I, J). As a result, H₂O₂-induced viability decrease (Fig. 6K), apoptosis (Fig. 6L), and necrosis (LDH releasing, Fig. 6M) were largely attenuated by Keap1 KO. Significantly, in Keap1 KO osteoblasts, Cpd16 (25 μM) was unable to further enhance Nrf2 activation (Fig. 6I, J). Neither did it offer additional cytoprotection against H₂O₂ (Fig. 6K–M). In ko-

Keap1 murine osteoblasts Cpd16 was unable to inhibit H₂O₂-induced viability decreasing (Fig. 6K), apoptosis (Fig. 6L), and medium LDH releasing (Fig. 6M). These results provided additional evidence to support that Nrf2 is indispensable for Cpd16-induced osteoblast cytoprotection.

### Keap1 Cys151S mutation abolishes Cpd16-induced Nrf2 cascade activation and osteoblasts protection
Cpd16 activated Nrf2 signaling by acting as the Keap1-Nrf2 protein–protein interaction inhibitor [54, 55]. However, the detailed mechanisms are still elusive. Therefore a Cys151S mutant Keap1 [56] vector was stably transduced to primary human osteoblasts. Keap1 (C151S) expression was confirmed in Fig. 7A. Importantly Cpd16-induced Nrf2 protein stabilization was largely inhibited by Keap1 mutation in human osteoblasts (Fig. 7A). Moreover, Cpd16-initiated expression of Nrf2-dependent genes was largely inhibited by the Keap1 mutation (Fig. 7B, C). As shown, H₂O₂-induced cell viability decreasing (Fig. 7D), apoptosis (Fig. 7E), and necrosis (Fig. 7F) were augmented in the Keap1-mutant human osteoblasts. Moreover, Cpd16-induced osteoblast cytoprotection against H₂O₂ was almost reversed in osteoblasts with the mutant Keap1 (Fig. 7D–F). These results implied that Keap1 cysteine (151) alkylatation could be vital for Cpd16-stimulated Nrf2 cascade activation, exerting osteoblast cytoprotection against H₂O₂.
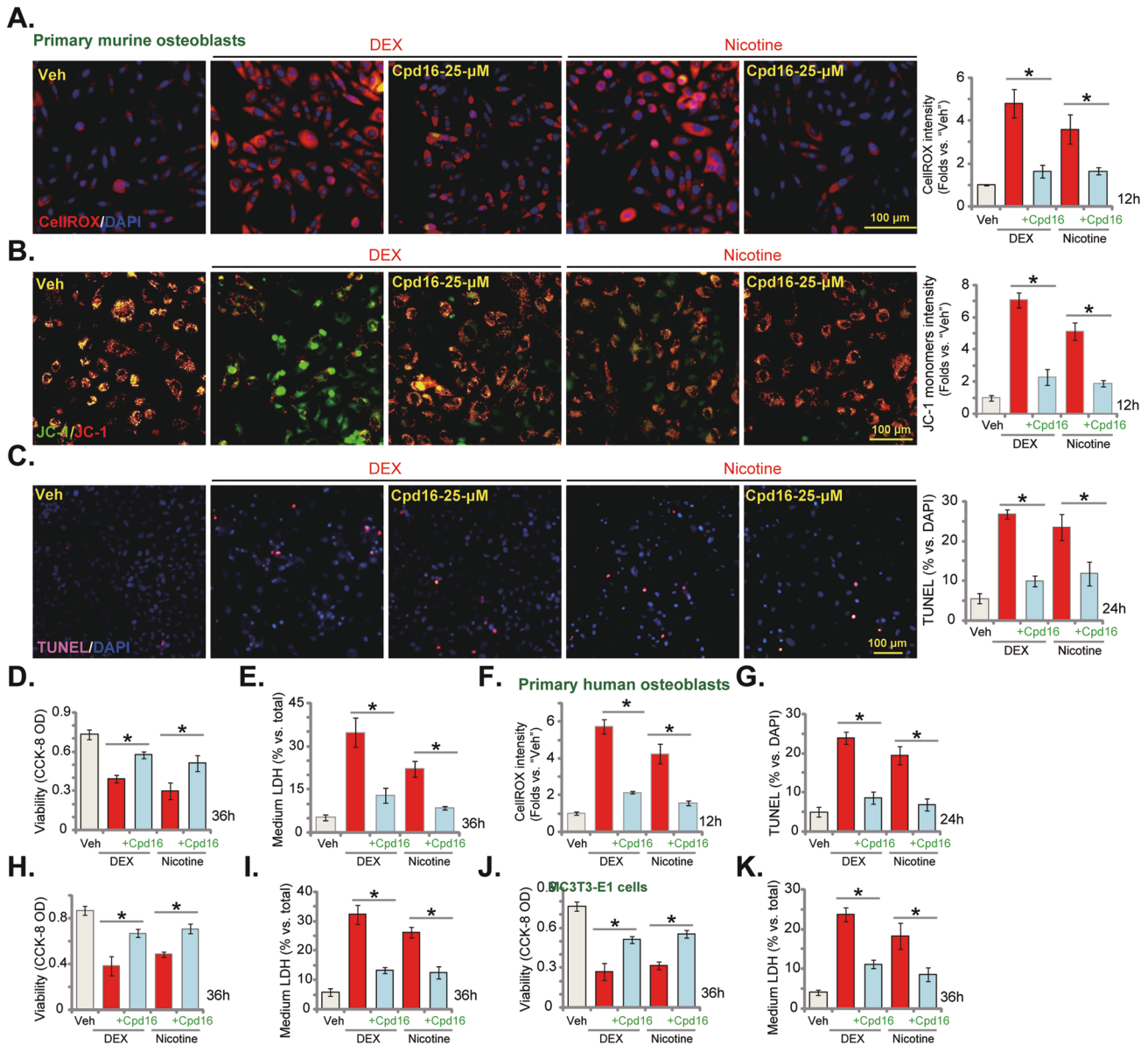
**Fig. 5 Cpd16 inhibits dexamethasone- and nicotine-induced oxidative injury in osteoblasts.** The primary murine osteoblasts (**A**–**E**), human osteoblasts (**F**–**I**), or the MC3T3-E1 murine osteoblastic cells (**J**, **K**) were pretreated (for 2 h) with Cpd16 (25 µM), followed with or without dexamethasone (DEX, 2 µM) or nicotine (1 µM) treatments, ROS, depolarization of mitochondria, apoptosis, viability, and necrosis were tested by CellROX staining (**A**, **F**), JC-1 staining (**B**), TUNEL-nuclei staining (**C**, **G**), CCK-8 (**D**, **H**, **J**), and LDH releasing (**E**, **I**, **K**) assays, respectively. $*P < 0.05$. Scale bar = 100 µm (**A**–**C**).

## Cpd16 administration largely ameliorates trabecular bone loss in OVX mice

To examine the potential activity by Cpd16 in vivo, the mouse OVX model was utilized. The representative micro-CT images demonstrated that weekly intraperitoneal injection of Cpd16 (5 mg/kg) largely ameliorated trabecular bone loss in the OVX mice (Fig. 8A). The reductions of BV/TV (%, Fig. 8B) and BMD (Fig. 8C) in trabecular bones of OVX mice were largely alleviated with Cpd16 administration. Moreover, BMD of the cortical bones was also slightly decreased eight weeks after OVX (Fig. 8D), which was also inhibited following Cpd16 administration (Fig. 8D). Whether the antioxidant mechanism was activated by Cpd16 in vivo was determined. As shown, the SOD activity in the left tibias was significantly decreased in OVX group mice (8 weeks after OVX, Fig. 8E), while Cpd16 administration remarkably elevated it (Fig. 8E). These results showed that Cpd16

administration largely ameliorated oxidative injury and trabecular bone loss in OVX mice.

## DISCUSSION

The transcription factor Nrf2 promotes the transcription and expression of a large number of antioxidant and/or defense genes, serving as a potential therapeutic target involved in the mitigation oxidative injury in osteoblasts [10, 13, 15, 16, 24, 28, 36]. Forced activation of Nrf2 signaling in osteoblasts/osteoblastic cells, using different agents or genetic strategies, was able to significantly inhibit oxidative injury by $H_2O_2$ and a number of other oxidative stimuli [10, 13, 15, 16, 24, 28, 36].

Here in different osteoblasts, Cpd16 treatment at only micromolar concentrations induced disassociation of Keap1-Nrf2, stabilization of Nrf2 protein and following nuclear translocation,
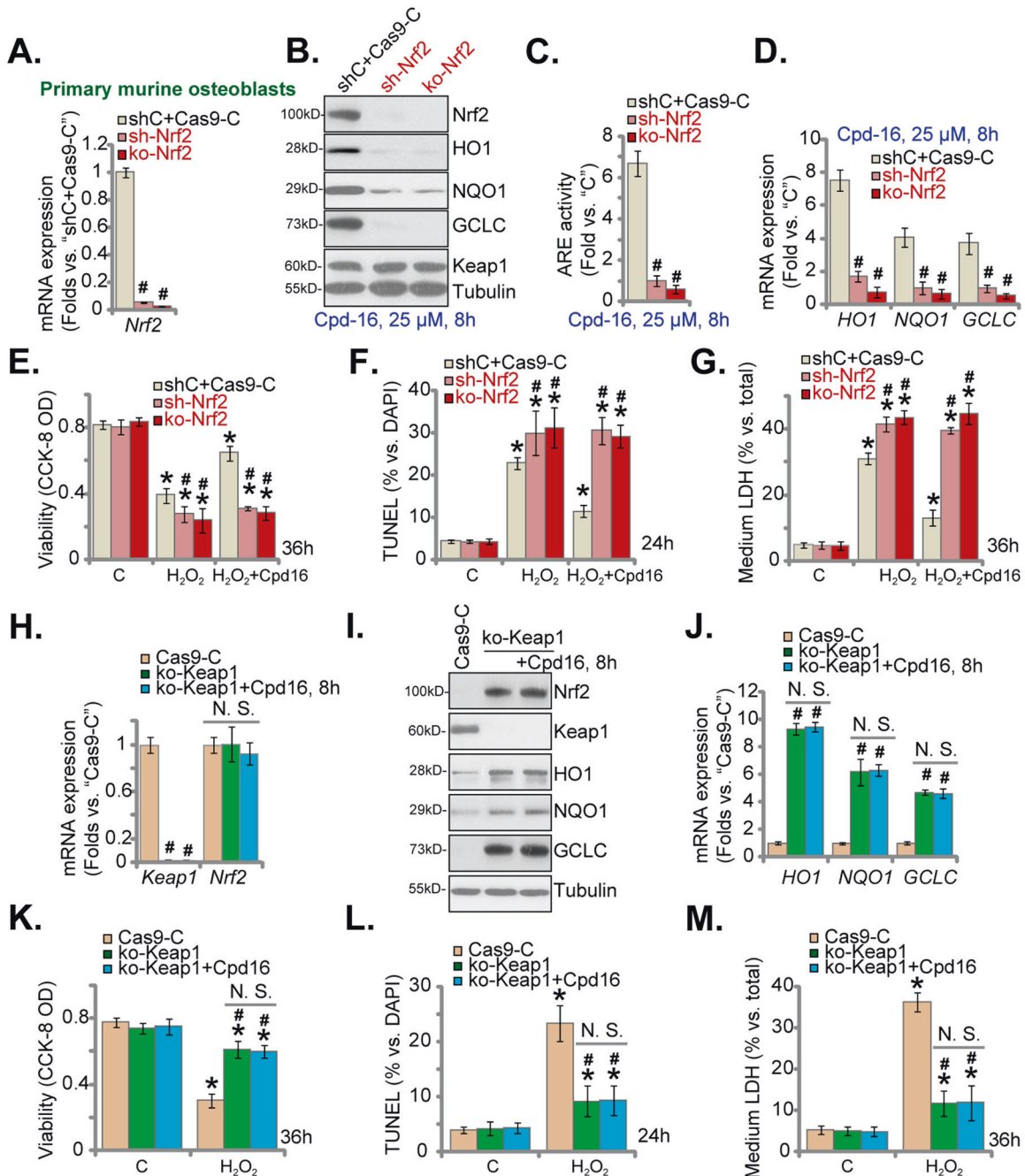
J. Zhao et al.



**Fig. 6  Nrf2 activation is indispensable for Cpd16-mediated osteoblast cytoprotection.** *Nrf2* mRNA expression in the listed primary murine osteoblasts was measured (**A**); the osteoblasts were treated with Cpd16, and listed proteins (**B**), ARE activity (**C**), and listed mRNAs (**D**) were measured; the murine osteoblasts were pretreated with Cpd16 (25 µM) for 2 h, followed by $H_2O_2$ (400 µM) stimulation, with cell viability, apoptosis and necrosis tested by CCK-8 (**E**), TUNEL-nuclei staining (**F**), and LDH releasing **G** assays, respectively. *Keap1-Nrf2* mRNA expression in the ko-Keap1 or Cas9-C murine osteoblasts was measured (**H**); the ko-Keap1 murine osteoblasts were also treated with or without Cpd16 (25 µM), expression of listed proteins and mRNAs (**I**, **J**) was measured; the ko-Keap1 osteoblasts were pretreated with Cpd16 (25 µM) for 2 h, followed by $H_2O_2$ (400 µM) stimulation; cell viability, apoptosis, and necrosis were measured by CCK-8 (**K**), TUNEL-nuclei (**L**), and LDH releasing **M** assays, respectively. *$P < 0.05$ versus "C" cells. #$P < 0.05$ versus "shC+Cas9-C"/"Cas9-C" osteoblasts. "N.S." stands for the non-statistical difference ($P > 0.05$).

and enhanced ARE reporter activity as well as transcription of Nrf2 response genes (*HO1*, *GCLC*, and *NQO1*) in cultured osteoblasts/osteoblastic cells. Significantly, Cpd16 ameliorated oxidative injury in $H_2O_2$-stimulated osteoblasts.

We found that Cpd16-induced Nrf2 activation and osteoblasts protection against $H_2O_2$ were stronger than other known Nrf2 activators (SFH, 4-OI, and TBHQ). One possibility is that Cpd16 could induce Keap1 cysteine (151) alkylatation, leading to

dramatic Keap1-Nrf2 disassociation and direct Nrf2 cascade activation. Indeed, we found that Keap1 Cys151S mutation abolished Cpd16-induced Nrf2 cascade activation and osteoblasts protection in primary human osteoblasts. The detailed mechanisms warrant further characterizations.

$H_2O_2$ and other oxidative stimuli (i.e. DEX), while activating cell apoptosis, can simultaneously induce programmed necrosis [10, 30, 57, 58]. The latter is a mitochondria-dependent active
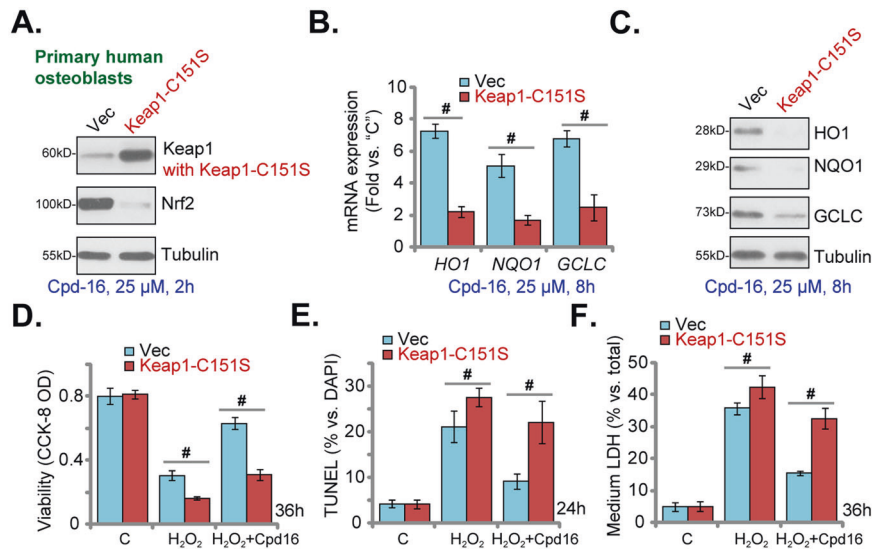
**Fig. 7 Keap1 Cys151S mutation abolishes Cpd16-induced Nrf2 cascade activation and osteoblasts cytoprotection.** Stable primary human osteoblasts with Cys151S Keap1 ("Keap1-C151S") or Vector were treated with Cpd16 (25 μM), listed proteins and genes were measured (**A–C**). Alternatively, the primary human osteoblasts were pretreated with Cpd16 (25 μM) for 2 h, followed by $H_2O_2$ (400 μM) stimulation, and cell viability, apoptosis, and necrosis were tested by CCK-8 (**D**), TUNEL-nuclei staining (**E**), and LDH releasing **F** assays, respectively. $^{\#}P < 0.05$.

and programmed cell necrosis cascade [10, 42, 59]. Oxidative stimuli can induce p53's translocation to mitochondria and form a multiple-protein complex with CyPD and ANT-1 [10, 42, 59]. The formation of the complex will thereafter induce mPTP open, mitochondrial depolarization, and cell necrosis [10, 42, 59]. Here, Cpd16 potently suppressed $H_2O_2$-stimulated programmed necrosis. $H_2O_2$-induced mitochondrial association of p53-CyPD-ANT1, depolarization of mitochondria, and cell necrosis were largely inhibited by Cpd16 pretreatment.

DEX can directly induce oxidative injury and osteoblast cell death, and it is a key factor for the progression of osteoporosis and osteonecrosis [60], which can be inhibited by Nrf2 activation [29, 50, 61]. Here DEX-caused oxidative injury and death in osteoblasts were largely attenuated by Cpd16. This novel Nrf2 small molecule activator should have promising value for the treatment of DEX-related bone injuries.

Sustained and/or high-dose nicotine exposure can significantly inhibit cell proliferation and differentiation in osteoblasts, and inhibit alkaline phosphatase (ALP) activity and collagen synthesis [51–53]. These changes together will eventually induce apoptosis, serving as the primary mechanism of cigarette smoke-related osteoporosis [51–53]. In the primary rat osteoblasts, nicotine was shown to inhibit multiple osteogenic and angiogenic genes [53]. We found that treatment with Cpd16 potently inhibited nicotine-induced oxidative injury and death of osteoblasts.

Osteoporosis seriously affects the life of the elderly people, especially postmenopausal women [62, 63]. One key pathophysiological feature of osteoporosis is osteoblast dysfunction, resulting in decreased bone formation [62, 63]. Oxidative stress-induced dysfunction and death of osteoblasts is the primary reason for the bone loss during the development of osteoporosis [64, 65]. Therefore, reducing oxidative stress, i.e. using Nrf2 activators, can protect osteoblasts and inhibit their death, which has a promising effect on improving osteoporosis [64, 65]. Here, Cpd16 inhibited $H_2O_2$-caused oxidative injury and death in cultured osteoblasts. The Nrf2 activator also largely ameliorated oxidative stress and trabecular bone loss in OVX mice. Therefore, it should have promising value for osteoporosis management.

## MATERIALS AND METHODS
### Reagents
Cpd16 was synthesized by Shanghai Ruilu Chemicals (Shanghai, China). Dexamethasone (DEX), nicotine, cycloheximide, Sulforaphane (SFH), 4-octyl itaconate (4-OI), tert-butylhydroquinone (TBHQ), MG-132, and hydrogen peroxide ($H_2O_2$) were purchased from Sigma (St Louis, MO). Antibodies were described early [30].

### Culture of primary murine/human osteoblasts and MC3T3-E1 murine osteoblastic cells
As described previously [10, 30], the trabecular bone fragments of written informed consent healthy donors were minced, washed, and digested. Thereafter, the primary human osteoblasts were obtained and cultivated in the described medium [30]. Medium was renewed twice a week. The primary murine osteoblasts were obtained and cultured as described [10, 30]. The established MC3T3-E1 cells were provided by Dr. Zhou and cultivated as reported [50]. The protocols were with approval from the Ethics Board of Shanghai Jiao Tong University School of Medicine.

### Genetic modifications in osteoblasts
For Nrf2 silencing, the lentiviral construct encoding short hairpin RNA (shRNA) sequence of Nrf2 [10, 30] was transduced to the primary murine osteoblasts. Following puromycin-mediated selection, the stable osteoblasts were formed. CRISPR/Cas9-induced knockout (KO) of Keap1 or Nrf2 as well as the establishment of the single stable osteoblasts were described previously [10, 30].

### Keap1 mutation
The GV248 lentiviral Cys151S mutant Keap1 construct (no GFP) was from Dr. Liu at Jiangsu University [66] and was stably transduced to the osteoblasts. Cys151S Keap1 was checked by western blotting.

Other assays, including cell viability CCK-8 assay, the Caspase-3/-9 activity, the JC-1 fluorescence testing mitochondrial depolarization, the CellROX fluorescence staining of ROS, the cell necrosis assay by measuring medium LDH contents, the lipid peroxidation by measuring the reactive substances (TBAR) activity, NQO1 activity assay, ARE reporter activity assay, and single strand DNA (ssDNA) ELISA as well as qRT-PCR, co-immunoprecipitation (Co-IP), western blotting, Annexin V flow cytometry and nuclear TUNEL staining assays were reported in the previous studies [10, 30]. Primers were provided by Dr. Jiang at Nanjing Medical University [67, 68]. The uncropped blotting images were presented in Figure S1.
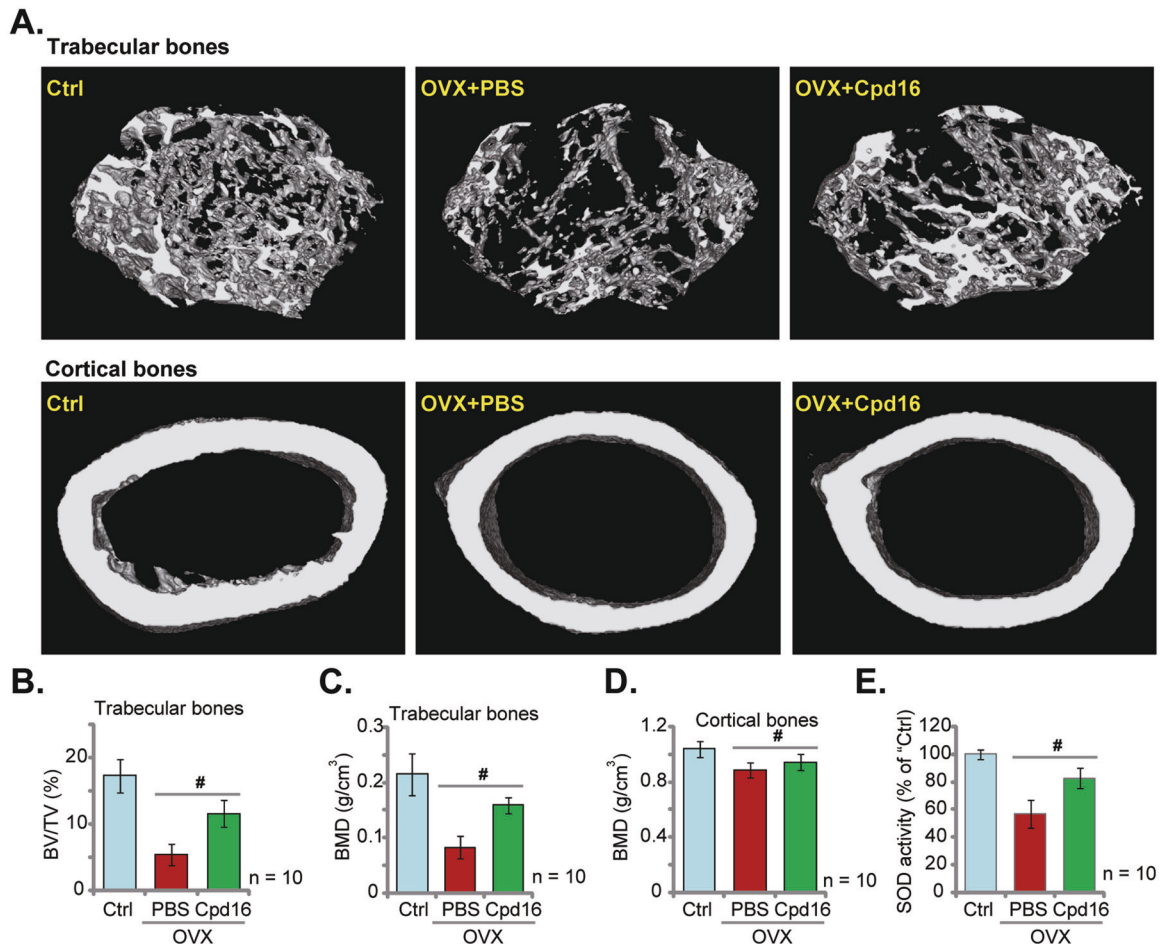
**Fig. 8 Cpd16 administration largely ameliorates trabecular bone loss in OVX mice.** The female C57/BL6 mice were subject to bilateral ovariectomy (OVX) procedure. Afterward, Cpd16 (at 5 mg/kg) or PBS were intraperitoneally injected (i.p.) at the first day of each week, and mice were sacrificed after 8 weeks. The representative micro-CT images of trabecular bones and cortical bones were presented (**A**). BV/TV (%, **B**) and bone mineral density (BMD, g/cm$^3$, **C**) of trabecular bones were calculated. BMD of cortical bones was recorded as well (**D**). The relative SOD activity in the left tibia bone tissues in different groups was shown (**E**). The control group mice were orally administered with PBS ("Ctrl"). 10 mice per group. $^\#P < 0.05$.

## The murine ovariectomized (OVX) procedure and micro-CT analyses

The female C57/BL6 mice, at 7 weeks of age and 21–22 g of weight, were purchased from SLAC (Shanghai, China). Mice were anesthetized as described [69] and the detailed protocols of OVX were reported early [69]. Cpd16 (5 mg/kg) or PBS was intraperitoneally injected (i.p.) at the first day of each week. Micro-CT analyses were described in an early study [70]. In brief, the OVX mice and the control mice were scanned under the micro-CT equipment (Skyscan 1176, Belgium) 8 weeks after OVX procedure and the high-resolution scanogram were retrieved [70]. The dataset was reconstructed under a CT analyzer software and bone erosion was calculated using the in-house Fiji script [70]. The trabecular bone volume (BV) versus the total volume (TV), in %, was measured. The bone mineral density (BMD, g/cm$^3$) of trabecular bones and cortical bones was calculated as well [70]. After completion of micro-CT, the right tibias of the mice were collected and superoxide dismutase (SOD) activity in the fresh bone tissues was analyzed by a SOD ELISA kit (Thermo-Fisher Invitrogen, Shanghai, China). All animal experiments were conducted under protocols approved by IACUC of Soochow University.

## Statistical analyses

Statistical analysis was described early [10, 30]. $P < 0.05$ was considered as a statistically significant difference. Quantified values were mean ± standard deviation (SD). All in vitro experiments were repeated five times and similar results were obtained.

## DATA AVAILABILITY

All data are available upon request.

## REFERENCES

1. Lewiecki EM. New targets for intervention in the treatment of postmenopausal osteoporosis. Nat Rev Rheumatol. 2011;7:631–8.
2. Harvey N, Dennison E, Cooper C. Osteoporosis: impact on health and economics. Nat Rev Rheumatol. 2010;6:99–105.
3. Dempster DW. Bone histomorphometry in glucocorticoid-induced osteoporosis. J Bone Min Res. 1989;4:137–41.
4. Zalavras CG, Lieberman JR. Osteonecrosis of the femoral head: evaluation and treatment. J Am Acad Orthop Surg. 2014;22:455–64.
5. Lieberman JR, Engstrom SM, Meneghini RM, SooHoo NF. Which factors influence preservation of the osteonecrotic femoral head? Clin Orthop Relat Res. 2012;470:525–34.
6. Mont MA, Jones LC, Hungerford DS. Nontraumatic osteonecrosis of the femoral head: ten years later. J Bone Jt Surg Am. 2006;88:1117–32.
7. Manolagas SC. From estrogen-centric to aging and oxidative stress: a revised perspective of the pathogenesis of osteoporosis. Endocr Rev. 2010;31:266–300.
8. Schroder K. NADPH oxidases in bone homeostasis and osteoporosis. Free Radic Biol Med. 2019;132:67–72.
9. Frenkel B, White W, Tuckermann J. Glucocorticoid-induced osteoporosis. Adv Exp Med Biol. 2015;872:179–215.
10. Zheng Y, Chen Z, She C, Lin Y, Hong Y, Shi L, et al. Four-octyl itaconate activates Nrf2 cascade to protect osteoblasts from hydrogen peroxide-induced oxidative injury. Cell Death Dis. 2020;11:772.

11. Liang J, Shen YC, Zhang XY, Chen C, Zhao H, Hu J. Circular RNA HIPK3 down-regulation mediates hydrogen peroxide-induced cytotoxicity in human osteoblasts. Aging. 2020;12:1159–70.

12. Ruan JW, Yao C, Bai JY, Zhou X Z microRNA-29a inhibition induces Gab1 upregulation to protect OB-6 human osteoblasts from hydrogen peroxide. Biochem Biophys Res Commun. 2018;503:607–14.

13. Xu D, Zhu H, Wang C, Zhu X, Liu G, Chen C, et al. microRNA-455 targets cullin 3 to activate Nrf2 signaling and protect human osteoblasts from hydrogen peroxide. Oncotarget 2017;8:59225–34.

14. Liu W, Mao L, Ji F, Chen F, Hao Y, Liu G. Targeted activation of AMPK by GSK621 ameliorates H2O2-induced damages in osteoblasts. Oncotarget 2017;8:10543–52.

15. Han D, Chen W, Gu X, Shan R, Zou J, Liu G, et al. Cytoprotective effect of chlorogenic acid against hydrogen peroxide-induced oxidative stress in MC3T3-E1 cells through PI3K/Akt-mediated Nrf2/HO-1 signaling pathway. Oncotarget 2017;8:14680–92.

16. Guo S, Fei HD, Ji F, Chen FL, Xie Y, Wang SG. Activation of Nrf2 by MIND4-17 protects osteoblasts from hydrogen peroxide-induced oxidative stress. Oncotarget 2017;8:105662–72.

17. Krajka-Kuzniak V, Paluszczak J, Baer-Dubowska W. The Nrf2-ARE signaling pathway: an update on its regulation and possible role in cancer prevention and treatment. Pharm Rep. 2017;69:393–402.

18. Suzuki T, Yamamoto M. Molecular basis of the Keap1-Nrf2 system. Free Radic Biol Med. 2015;88:93–100.

19. Keum YS, Choi BY. Molecular and chemical regulation of the Keap1-Nrf2 signaling pathway. Molecules 2014;19:10074–89.

20. Ma Q, He X. Molecular basis of electrophilic and oxidative defense: promises and perils of Nrf2. Pharm Rev. 2012;64:1055–81.

21. Kundu JK, Surh YJ. Nrf2-Keap1 signaling as a potential target for chemoprevention of inflammation-associated carcinogenesis. Pharm Res. 2010;27:999–1013.

22. Cheng J, Wang H, Zhang Z, Liang K. Stilbene glycoside protects osteoblasts against oxidative damage via Nrf2/HO-1 and NF-kappaB signaling pathways. Arch Med Sci. 2019;15:196–203.

23. Xia G, Li X, Zhu X, Yin X, Ding H, Qiao Y. Mangiferin protects osteoblast against oxidative damage by modulation of ERK5/Nrf2 signaling. Biochem Biophys Res Commun. 2017;491:807–13.

24. Lee D, Kook SH, Ji H, Lee SA, Choi KC, Lee KY, et al. N-acetyl cysteine inhibits H2O2-mediated reduction in the mineralization of MC3T3-E1 cells by downregulating Nrf2/HO-1 pathway. BMB Rep. 2015;48:636–41.

25. Xu YY, Chen FL, Ji F, Fei HD, Xie Y, Wang SG. Activation of AMP-activated protein kinase by compound 991 protects osteoblasts from dexamethasone. Biochem Biophys Res Commun. 2018;495:1014–21.

26. Liu G, Chen FL, Ji F, Fei HD, Xie Y, Wang S G microRNA-19a protects osteoblasts from dexamethasone via targeting TSC1. Oncotarget 2018;9:2017–27.

27. Fan JB, Zhang Y, Liu W, Zhu XH, Xu DW, Zhao JN, et al. Long non-coding RNA MALAT1 protects human osteoblasts from dexamethasone-induced injury via activation of PPM1E-AMPK signaling. Cell Physiol Biochem. 2018;51:31–45.

28. Zhao S, Mao L, Wang SG, Chen FL, Ji F, Fei HD. MicroRNA-200a activates Nrf2 signaling to protect osteoblasts from dexamethasone. Oncotarget 2017;8:104867–76.

29. Liu W, Mao L, Ji F, Chen F, Wang S, Xie Y. Icariside II activates EGFR-Akt-Nrf2 signaling and protects osteoblasts from dexamethasone. Oncotarget 2017;8:2594–603.

30. Zheng YH, Yang JJ, Tang PJ, Zhu Y, Chen Z, She C, et al. A novel Keap1 inhibitor iKeap1 activates Nrf2 signaling and ameliorates hydrogen peroxide-induced oxidative injury and apoptosis in osteoblasts. Cell Death Dis. 2021;12:679.

31. Liang JQ, Zhou ZT, Bo L, Tan HN, Hu JH, Tan MS. Phosphoglycerate kinase 1 silencing by a novel microRNA microRNA-4523 protects human osteoblasts from dexamethasone through activation of Nrf2 signaling cascade. Cell Death Dis. 2021;12:964.

32. Zhuang Y, Wang S, Fei H, Ji F, Sun P. miR-107 inhibition upregulates CAB39 and activates AMPK-Nrf2 signaling to protect osteoblasts from dexamethasone-induced oxidative injury and cytotoxicity. Aging. 2020;12:11754–67.

33. Marcotte D, Zeng W, Hus JC, McKenzie A, Hession C, Jin P, et al. Small molecules inhibit the interaction of Nrf2 and the Keap1 Kelch domain through a non-covalent mechanism. Bioorg Med Chem. 2013;21:4011–9.

34. Mao J, Xia Q, Liu C, Ying Z, Wang H, Wang G. A critical role of Hrd1 in the regulation of optineurin degradation and aggresome formation. Hum Mol Genet. 2017;26:1877–89.

35. Li W, Kong AN. Molecular mechanisms of Nrf2-mediated antioxidant response. Mol Carcinog. 2009;48:91–104.

36. Liang J, Zhang XY, Zhen YF, Chen C, Tan H, Hu J, et al. PGK1 depletion activates Nrf2 signaling to protect human osteoblasts from dexamethasone. Cell Death Dis. 2019;10:888.

37. Park C, Lee H, Han MH, Jeong JW, Kim SO, Jeong SJ, et al. Cytoprotective effects of fermented oyster extracts against oxidative stress-induced DNA damage and apoptosis through activation of the Nrf2/HO-1 signaling pathway in MC3T3-E1 osteoblasts. EXCLI J. 2020;19:1102–19.

38. Han D, Gu X, Gao J, Wang Z, Liu G, Barkema HW, et al. Chlorogenic acid promotes the Nrf2/HO-1 anti-oxidative pathway by activating p21(Waf1/Cip1) to resist dexamethasone-induced apoptosis in osteoblastic cells. Free Radic Biol Med. 2019;137:1–12.

39. Yang L, Wu Z, Yin G, Liu H, Guan X, Zhao X, et al. Stem cell factor (SCF) protects osteoblasts from oxidative stress through activating c-Kit-Akt signaling. Biochem Biophys Res Commun. 2014;455:256–61.

40. She C, Zhu LQ, Zhen YF, Wang XD, Dong QR. Activation of AMPK protects against hydrogen peroxide-induced osteoblast apoptosis through autophagy induction and NADPH maintenance: new implications for osteonecrosis treatment? Cell Signal. 2014;26:1–8.

41. Qin LS, Jia PF, Zhang ZQ, Zhang SM. ROS-p53-cyclophilin-D signaling mediates salinomycin-induced glioma cell necrosis. J Exp Clin Cancer Res. 2015;34:57.

42. Vaseva AV, Marchenko ND, Ji K, Tsirka SE, Holzmann S, Moll UM. p53 opens the mitochondrial permeability transition pore to trigger necrosis. Cell 2012;149:1536–48.

43. Nakagawa T, Shimizu S, Watanabe T, Yamaguchi O, Otsu K, Yamagata H, et al. Cyclophilin D-dependent mitochondrial permeability transition regulates some necrotic but not apoptotic cell death. Nature 2005;434:652–8.

44. Tang C, Tan S, Zhang Y, Dong L, Xu Y. Activation of Keap1-Nrf2 signaling by 4-octyl itaconate protects human umbilical vein endothelial cells from high glucose. Biochem Biophys Res Commun. 2019;508:921–7.

45. Tang C, Wang X, Xie Y, Cai X, Yu N, Hu Y, et al. 4-Octyl itaconate activates Nrf2 signaling to inhibit pro-inflammatory cytokine production in peripheral blood mononuclear cells of systemic lupus erythematosus patients. Cell Physiol Biochem. 2018;51:979–90.

46. Chen X, Jiang Z, Zhou C, Chen K, Li X, Wang Z, et al. Activation of Nrf2 by sulforaphane inhibits high glucose-induced progression of pancreatic cancer via AMPK dependent signaling. Cell Physiol Biochem. 2018;50:1201–15.

47. Ping Z, Liu W, Kang Z, Cai J, Wang Q, Cheng N, et al. Sulforaphane protects brains against hypoxic-ischemic injury through induction of Nrf2-dependent phase 2 enzyme. Brain Res. 2010;1343:178–85.

48. Zhao YL, Zhao W, Liu M, Liu L, Wang Y. TBHQ-overview of multiple mechanisms against oxidative stress for attenuating methamphetamine-induced neurotoxicity. Oxid Med Cell Longev. 2020;2020:8874304.

49. Li J, Johnson D, Calkins M, Wright L, Svendsen C, Johnson J. Stabilization of Nrf2 by tBHQ confers protection against oxidative stress-induced cell death in human neural stem cells. Toxicol Sci. 2005;83:313–28.

50. Li ST, Chen NN, Qiao YB, Zhu WL, Ruan JW, Zhou XZ. SC79 rescues osteoblasts from dexamethasone though activating Akt-Nrf2 signaling. Biochem Biophys Res Commun. 2016;479:54–60.

51. Marinucci L, Balloni S, Fettucciari K, Bodo M, Talesa VN, Antognelli C. Nicotine induces apoptosis in human osteoblasts via a novel mechanism driven by $H_2O_2$ and entailing Glyoxalase 1-dependent MG-H1 accumulation leading to TG2-mediated NF-kB desensitization: Implication for smokers-related osteoporosis. Free Radic Biol Med. 2018;117:6–17.

52. Liang D, Wang KJ, Tang ZQ, Liu RH, Zeng F, Cheng MY, et al. Effects of nicotine on the metabolism and gene expression profile of SpragueDawley rat primary osteoblasts. Mol Med Rep. 2018;17:8269–81.

53. Ma L, Zwahlen RA, Zheng LW, Sham MH. Influence of nicotine on the biological activity of rabbit osteoblasts. Clin Oral Implants Res. 2011;22:338–42.

54. Leung CH, Zhang JT, Yang GJ, Liu H, Han QB, Ma DL. Emerging screening approaches in the development of Nrf2-Keap1 protein-protein interaction inhibitors. Int J Mol Sci. 20, 4445 (2019).

55. Zhuang C, Wu Z, Xing C, Miao Z. Small molecules inhibiting Keap1-Nrf2 protein-protein interactions: a novel approach to activate Nrf2 function. Medchemcomm 2017;8:286–94.

56. Mills EL, Ryan DG, Prag HA, Dikovskaya D, Menon D, Zaslona Z, et al. Itaconate is an anti-inflammatory metabolite that activates Nrf2 via alkylation of KEAP1. Nature 2018;556:113–7.

57. Zhu CY, Yao C, Zhu LQ, She C, Zhou XZ. Dexamethasone-induced cytotoxicity in human osteoblasts is associated with circular RNA HIPK3 downregulation. Biochem Biophys Res Commun. 2019;516:645–52.

58. Hong H, Sun Y, Deng H, Yuan K, Chen J, Liu W, et al. Dysregulation of cPWWP2A-miR-579 axis mediates dexamethasone-induced cytotoxicity in human osteoblasts. Biochem Biophys Res Commun. 2019;517:491–8.

59. Montero J, Dutta C, van Bodegom D, Weinstock D, Letai A. p53 regulates a non-apoptotic death induced by ROS. Cell Death Differ. 2013;20:1465–74.

60. Polderman JA, Farhang-Razi V, Van Dieren S, Kranke P, DeVries JH, Hollmann MW, et al. Adverse side effects of dexamethasone in surgical patients. Cochrane Database Syst Rev. 2018;11:CD011940.

61. Ji F, Hu X, Hu W, Hao YD. FGF23 protects osteoblasts from dexamethasone-induced oxidative injury. Aging. 2020;12:19045–59.

62. Reid IR, Billington EO. Drug therapy for osteoporosis in older adults. Lancet 2022;399:1080–92.

63. Rachner TD, Khosla S, Hofbauer LC. Osteoporosis: now and the future. Lancet 2011;377:1276–87.

64. Kimball JS, Johnson JP, Carlson DA. Oxidative stress and osteoporosis. J Bone Jt Surg Am. 2021;103:1451–61.

65. Zhou Q, Zhu L, Zhang D, Li N, Li Q, Dai P, et al. Oxidative stress-related biomarkers in postmenopausal osteoporosis: a systematic review and meta-analyses. Dis Markers. 2016;2016:7067984.

66. Liu H, Feng Y, Xu M, Yang J, Wang Z, Di G. Four-octyl itaconate activates Keap1-Nrf2 signaling to protect neuronal cells from hydrogen peroxide. Cell Commun Signal. 2018;16:81.

67. Xu XZ, Tang Y, Cheng LB, Yao J, Jiang Q, Li KR, et al. Targeting Keap1 by miR-626 protects retinal pigment epithelium cells from oxidative injury by activating Nrf2 signaling. Free Radic Biol Med. 2019;143:387–96.

68. Tang CZ, Li KR, Yu Q, Jiang Q, Yao J, Cao C. Activation of Nrf2 by Ginsenoside Rh3 protects retinal pigment epithelium cells and retinal ganglion cells from UV. Free Radic Biol Med. 2018;117:238–46.

69. Chen JR, Lazarenko OP, Zhao H, Wankhade UD, Pedersen K, Watt J, et al. Nox4 expression is not required for OVX-induced osteoblast senescence and bone loss in mice. JBMR. 2020;4:e10376.

70. Zhou Y, Deng Y, Liu Z, Yin M, Hou M, Zhao Z, et al. Cytokine-scavenging nano-decoys reconstruct osteoclast/osteoblast balance toward the treatment of post-menopausal osteoporosis. Sci Adv. 2021;7:eabl6432.

## AUTHOR CONTRIBUTIONS

All the listed authors designed the study, performed the experiments and the statistical analysis, and wrote the manuscript and revise it. All the listed authors have read the manuscript and approved the final version.

## COMPETING INTERESTS

The authors declare no competing interests.

## ETHICS STATEMENT

This study was approved by the Ethics Committee of Shanghai Jiao Tong University School of Medicine.

## ADDITIONAL INFORMATION

**Supplementary information** The online version contains supplementary material available at https://doi.org/10.1038/s41420-022-01146-7.

**Correspondence** and requests for materials should be addressed to Quan Li, Ke-ran Li or Yue-huan Zheng.

**Reprints and permission information** is available at http://www.nature.com/reprints

**Publisher's note** Springer Nature remains neutral with regard to jurisdictional claims in published maps and institutional affiliations.